Thai Journal of Mathematics
Volume 12 (2014) Number 1 : 207–221
http://thaijmath.in.cmu.ac.th
ISSN 1686-0209

Natural Convection in Porous Square Cavities with Discrete Heat Sources on Bottom and Side Walls

Wiratchada Kalaoka and Supot Witayangkurn[1]

Department of Mathematics, Faculty of Science
Khon Kaen University, Khon Kaen 40002, Thailand
e-mail : wiratchadakalaoka@gmail.com (W. Kalaoka)
supot_wa@kku.ac.th (S. Witayangkurn)

Abstract : A numerical study of natural convection flow in porous square cavities with discrete heat sources is studied in this paper. Two cases depending on varying the positions of discrete heat sources on the walls are considered. For case 1, two heat sources are located at the lower portion on the side walls while they are located at the upper for case 2. Both of case 1 and case 2, there is one heat source located at the center portion on the bottom wall and the top wall is adiabatic. The study is performed for different Darcy numbers, ($Da = 10^{-4} - 10^{-2}$) while Rayleigh number ($Ra = 10^5$) and Prandtl number ($Pr = 0.72$) are kept constant. FlexPDE 6.14 student version is used to solve the governing equations which is based on the finite element method. The results are displayed in the terms of isotherms, streamlines and heatlines. It is found that the temperature distribution is more distributed in the cavities. The strength of convection is stronger as seen from the greater magnitudes of streamfunctions. Thermal mixing is intensified which is shown by the formation of heatlines cells.

Keywords : discrete heat sources; finite element method; natural convection; porous media.
2010 Mathematics Subject Classification : 65M60; 76R10; 76S05.

[1]Corresponding author.

Notations

Da	Darcy number	x, y	distance along x and y coordinates (m)
g	acceleration due to gravity (ms^{-2})	X, Y	dimensionless distance along x and y coordinates
K	permeability of porous medium (m^2)	*Greek symbols*	
L	size of the square cavity (m)	α	thermal diffusivity (m^2s^{-1})
p	pressure (Pa)	β	volume expansion coefficient (K^{-1})
P	dimensionless pressure	γ	penalty parameter
Pr	Prandtl number	θ	dimensionless temperature
Ra	Rayleigh number	ν	kinematic viscosity (m^2s^{-1})
T	temperature (K)	ρ	density (kgm^{-3})
T_h	temperature of discrete heat sources (K)	Ψ	streamfunction
T_c	temperature of cold portions of the cavity (K)	Π	heatfunction
u, v	x and y components of velocity (ms^{-1})	*Subscripts*	
U, V	x and y components of dimensionless velocity	c	cold wall
		h	hot wall

1 Introduction

Analysis of natural convection flow filled with a porous media has received attention in the past year. This interest is due to a number of technical applications, such as separation processes in chemical industries, fluid flow in geothermal reservoirs, dispersion of chemical contaminants through water saturated soil, migration of moisture in grain storage system, crude oil production, solidification of casting, etc.

Natural convection in discretely heated porous enclosures has been studied extensively. El-Khatib and Prasad [1] studied the effects of stratification on thermal convection in horizontal porous layers with a localized heat source on bottom surface and linearly varying temperature on vertical walls. Robillard [2] investigated multiple steady states in a confined porous medium with localized heating from below whereas an upper surface is cool and the other surfaces is adiabatic. Free and mixed convection in horizontal porous layers heated from below by multiple, isothermal, discrete heat source for different Rayleigh and Peclet numbers have been carried out by Lai et al. [3, 4]. Further, Heindel et al. [5] reported experimental and numerical studies on natural convection heat transfer from the fin arrys of discrete heat sources filled with a porous medium. Saeid and Pop [6] studied the natural convection in a porous square enclosure with isothermal discrete heater on one of the vertical walls and the other vertical wall is kept constant temperature, while the horizontal walls are adiabatic. Zhao et al. [7] reported a

numerical study on double-diffusive convective flow of a binary mixture in a porous enclosure subject to localized heating and salting from one side. Recently, Sankar et al. [8] studied the natural convection flows in a vertical annulus filled with a fluid-saturated porous medium.

This study is the problem on two-dimensional natural convection inside porous square enclosures using finite element method. Two different cases with various the locations of discrete heat sources on the walls of the cavities are considered. The objective of the present paper is to investigate the flow field, temperature distribution and heat flow in the enclosures. Main attention is focused on the effect of Darcy numbers. The interested parameters are Darcy numbers ($10^{-4} \leq Da \leq 10^{-2}$), Prandtl number ($Pr = 0.72$) and Rayleigh number ($Ra = 10^5$).

2 Simulation and mathematical formulation

The physical domains of two cases are depicted in Figure 1. These domains consist of porous square cavities with discrete isothermal heating, which are displayed by thick lines. In all the cases, the heat source is fixed at the center of the bottom wall. Figure 1(a) shows the heat sources are placed at the lower portions on the vertical walls and Figure 1(b) shows the heat sources are placed at the upper portions on the vertical walls. The top wall is insulated. The dimensionless length of the heat sources on the bottom wall is 0.20 while that on the vertical walls is 0.40.

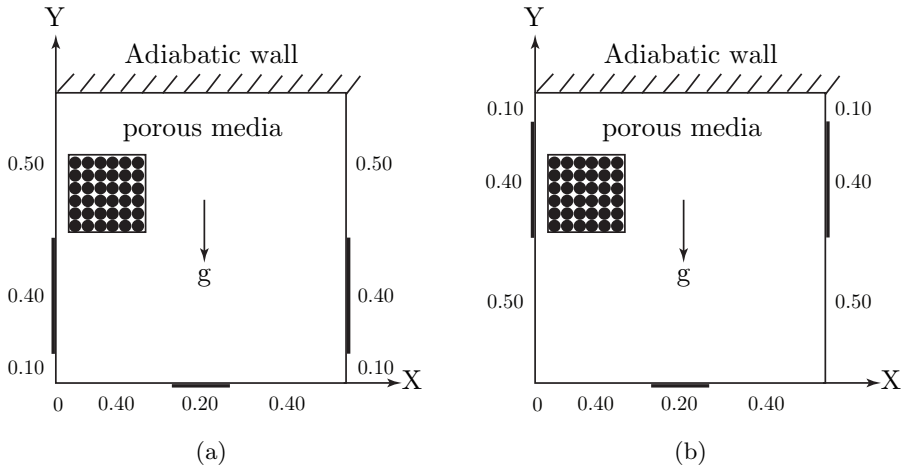

Figure 1: Physical domains of the enclosures for different cases: (a) case 1 and (b) case 2.

All the physical properties are assumed to be constant except the density in buoyancy term. Change in density due to temperature variation is calculated

using Boussinesq approximation. Another important assumption is that the local thermal equilibrium (LTE) is valid [9, 10]. The governing equations for steady two-dimensional natural convection flow in porous square enclosures using conversation of mass, momentum and energy can be written as

$$\frac{\partial u}{\partial x}+\frac{\partial u}{\partial y}=0, \tag{2.1}$$

$$u\frac{\partial u}{\partial x}+v\frac{\partial u}{\partial y}=-\frac{\partial p}{\partial x}+\nu\left(\frac{\partial^2 u}{\partial x^2}+\frac{\partial^2 u}{\partial y^2}\right)-\frac{\nu}{K}u, \tag{2.2}$$

$$u\frac{\partial v}{\partial x}+v\frac{\partial v}{\partial y}=-\frac{\partial p}{\partial x}+\nu\left(\frac{\partial^2 v}{\partial x^2}+\frac{\partial^2 v}{\partial y^2}\right)-\frac{\nu}{K}v+g\beta(T-T_c), \tag{2.3}$$

$$u\frac{\partial T}{\partial x}+v\frac{\partial T}{\partial y}=\alpha\left(\frac{\partial^2 T}{\partial x^2}+\frac{\partial^2 T}{\partial y^2}\right). \tag{2.4}$$

The above governing equations are transformed to dimensionless form by using the following change of variables:

$$\left.\begin{aligned} X=\frac{x}{L},\quad Y=\frac{y}{L},\quad U=\frac{uL}{\alpha},\quad V=\frac{vL}{\alpha},\quad \theta=\frac{T-T_c}{T_h-T_c},\\ P=\frac{pL^2}{\rho\alpha^2},\quad Pr=\frac{\nu}{\alpha},\quad Da=\frac{K}{L^2},\quad Ra=\frac{g\beta(T_h-T_c)L^3Pr}{\nu^2}. \end{aligned}\right\} \tag{2.5}$$

The governing equations (2.1)-(2.4) reduce to the following non-dimensional form:

$$\frac{\partial U}{\partial X}+\frac{\partial U}{\partial Y}=0, \tag{2.6}$$

$$U\frac{\partial U}{\partial X}+V\frac{\partial U}{\partial Y}=-\frac{\partial P}{\partial X}+Pr\left(\frac{\partial^2 U}{\partial X^2}+\frac{\partial^2 U}{\partial Y^2}\right)-\frac{Pr}{Da}U, \tag{2.7}$$

$$U\frac{\partial V}{\partial X}+V\frac{\partial V}{\partial Y}=-\frac{\partial P}{\partial Y}+Pr\left(\frac{\partial^2 V}{\partial X^2}+\frac{\partial^2 V}{\partial Y^2}\right)-\frac{Pr}{Da}V+RaPr\theta, \tag{2.8}$$

$$U\frac{\partial \theta}{\partial X}+V\frac{\partial \theta}{\partial Y}=\frac{\partial^2 \theta}{\partial X^2}+\frac{\partial^2 \theta}{\partial Y^2}. \tag{2.9}$$

In order to solve the equations (2.7)-(2.8) by eliminating the pressure, we use the penalty finite element method with a penalty parameter such that [11]

$$P=-\gamma\left(\frac{\partial U}{\partial X}+\frac{\partial V}{\partial Y}\right). \tag{2.10}$$

Typical values of γ that yield consistent solutions are 10^7. Substituting (2.10) into (2.7) and (2.8), we have

$$\begin{aligned} U\frac{\partial U}{\partial X}+V\frac{\partial U}{\partial Y}=\gamma\frac{\partial}{\partial X}\left(\frac{\partial U}{\partial X}+\frac{\partial V}{\partial Y}\right)+Pr\left(\frac{\partial^2 U}{\partial X^2}+\frac{\partial^2 U}{\partial Y^2}\right)\\ -\frac{Pr}{Da}U, \end{aligned} \tag{2.11}$$

and

$$U\frac{\partial V}{\partial X}+V\frac{\partial V}{\partial Y}=\gamma\frac{\partial}{\partial Y}\left(\frac{\partial U}{\partial X}+\frac{\partial V}{\partial Y}\right)+Pr\left(\frac{\partial^2 V}{\partial X^2}+\frac{\partial^2 V}{\partial Y^2}\right)-\frac{Pr}{Da}V+RaPr\theta. \tag{2.12}$$

The boundary conditions for velocities with cases $1-2$ are

$$\begin{aligned} U(X,0)=U(X,1)=U(0,Y)=U(1,Y)=0,\\ V(X,0)=V(X,1)=V(0,Y)=V(1,Y)=0. \end{aligned} \tag{2.13}$$

The boundary conditions for temperature are

$$\left.\begin{aligned} \text{for hot regime}: \theta=1,\\ \text{for cold regime}: \theta=0,\\ \text{for adiabatic top wall}: \frac{\partial\theta}{\partial Y}=0. \end{aligned}\right\} \tag{2.14}$$

2.1 Streamfunction and heatfunction

2.1.1 Streamfunction

The streamfunction (ψ) is used to visualize the convective fluid flow within the enclosures. The dimensionless streamfunction is defined as $U=\frac{\partial\psi}{\partial Y}$ and $V=-\frac{\partial\psi}{\partial X}$ [12]. Therefore the equation (2.6) is changed to (2.15)

$$\frac{\partial^2\psi}{\partial X^2}+\frac{\partial^2\psi}{\partial Y^2}=\frac{\partial U}{\partial Y}-\frac{\partial V}{\partial X}. \tag{2.15}$$

The boundary condition for streamfunction is

$$\psi=0. \tag{2.16}$$

2.1.2 Heatfunction

The heatfunction (Π) is used to visualize the heat flow within the enclosures. The dimensionless heatfunction is defined as $\frac{\partial\Pi}{\partial Y}=U\theta-\frac{\partial\theta}{\partial X}$ and $-\frac{\partial\Pi}{\partial X}=V\theta-\frac{\partial\theta}{\partial Y}$ [13]. Thus, the equation (2.9) is changed to (2.17)

$$\frac{\partial^2\Pi}{\partial X^2}+\frac{\partial^2\Pi}{\partial Y^2}=\frac{\partial}{\partial Y}(U\theta)-\frac{\partial}{\partial X}(V\theta). \tag{2.17}$$

The boundary conditions for heatfunction are

$$\left.\begin{aligned} \text{for hot regime on bottom wall} : \tfrac{\partial \Pi}{\partial Y} &= \pi\cos(\pi X),\\ \text{for hot regime on side walls} : \tfrac{\partial \Pi}{\partial X} &= -\pi\cos(\pi Y) \text{ or } \pi\cos(\pi Y),\\ \text{for cold regime on bottom wall} : \tfrac{\partial \Pi}{\partial Y} &= 0,\\ \text{for cold regime on side walls} : \tfrac{\partial \Pi}{\partial X} &= 0,\\ \text{for adiabatic wall} : \Pi &= 0. \end{aligned}\right\} \tag{2.18}$$

3 Results and discussion

The discussions and the numerical results for the problem of natural convection in porous square enclosures with various sections of discrete heat sources are presented in this section. The procedure mentioned previously is coded into FlexPDE 6.14 student version. The computations are carried out for a wide range of Darcy numbers ($10^{-4} \leq Da \leq 10^{-2}$) such that Prandtl number and Rayleigh number are kept constant at 0.72 and 10^5, respectively. The flow, temperature and heat fields are displayed in terms of isotherms streamlines and heatlines.

3.1 Case 1

The schematic diagram for case 1 is shown in Figure 1(a). The heat sources are placed at the center portion of the bottom wall ($0.40 \leq X \leq 0.60$) and the lower portion of the vertical walls ($0.10 \leq Y \leq 0.50$). Detailed computations have been carried out for Darcy numbers, $Da = 10^{-4}, 10^{-3}$ and 10^{-2} while Rayleigh number and Prandtl number are fixed at $Ra = 10^5$ and $Pr = 0.72$, respectively.

At $Da = 10^{-4}$, isotherms are smooth and they are symmetric near the top portion of the side walls for $\theta = 0.10$. Values of isotherms at the center core are $\theta = 0.20 - 0.40$ and the isotherms disperse near the bottom corner for $\theta = 0.10 - 0.40$. When Da is increased to 10^{-3}, it is noted that isotherm with $\theta = 0.20$ disperses to the top portion of the vertical walls as seen from Figure 2(b). Isotherms at $\theta = 0.30 - 0.40$ are found to be compress along the vertical walls as Da is increased to 10^{-2}.

At $Da = 10^{-4}$, the circulation cells of streamlines are weak. It may be noted that the multiple circulations are formed in the cavity and the primary circulation is bi-cellular as seen in Figure 3(a). For $Da = 10^{-3}$, the flow direction is similar to the case of $Da = 10^{-4}$ but the intensity is stronger as shown in Figure 3(b). In addition, the smallest circulations at the lower portion of the cavity are disappear. The bi-cellular in the primary circulation disappear and the strength of fluid motion is enhanced with $|\psi|_{max} = 5.00$ when Da is increased to 10^{-2}.

The heatlines illustrated in Figure 4(a) are wavy and they are dispersed near the lower of side walls due to the locations of discrete heat sources for $Da = 10^{-4}$. As Da is incresed to $= 10^{-3}$, the less heatlines are remain dispersed near the low

portion of the side walls. The heatlines presented in Figure 4(c) show that the multiple circulations are occurred in the enclosure with $Da = 10^{-2}$.

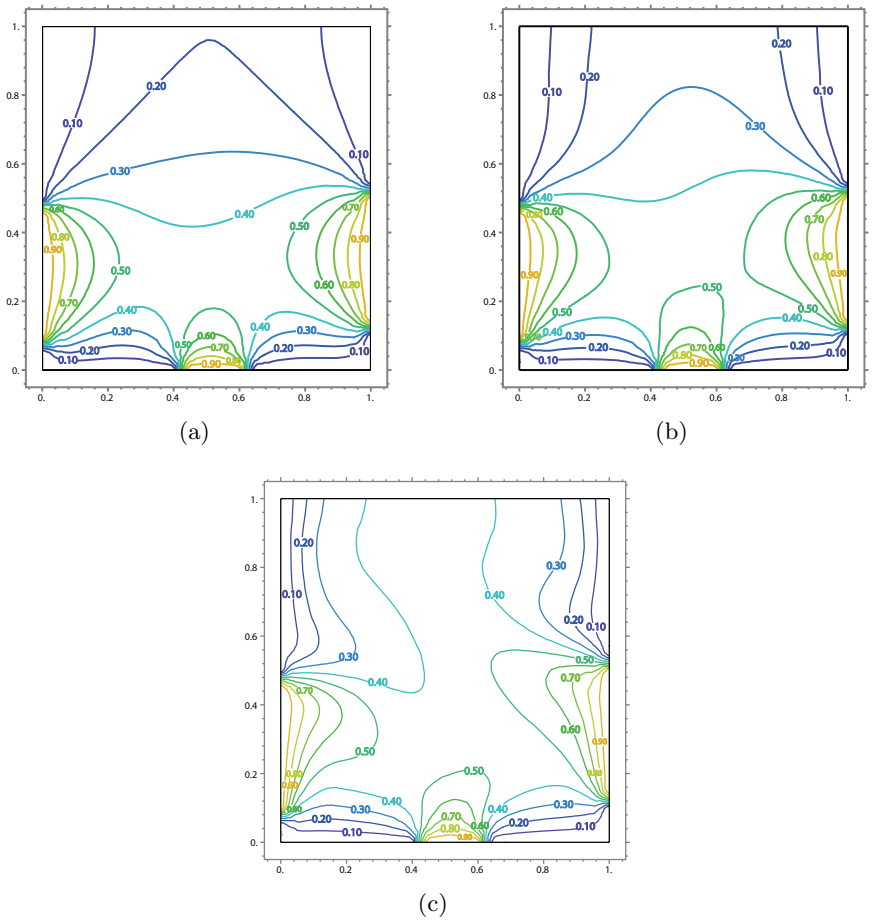

Figure 2: Isotherms for case 1 with $Ra = 10^5$, $Pr = 0.72$ and (a) $Da = 10^{-4}$ (b) $Da = 10^{-3}$ and (c) $Da = 10^{-2}$.

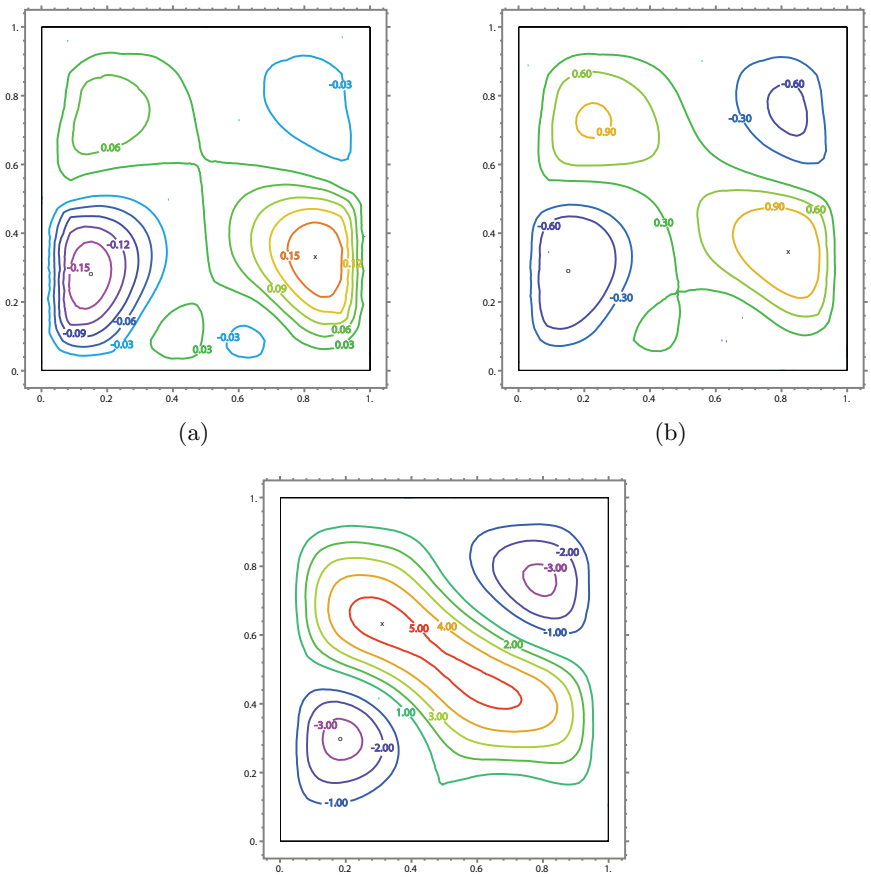

Figure 3: Streamlines for case 1 with $Ra = 10^5$, $Pr = 0.72$ and (a) $Da = 10^{-4}$ (b) $Da = 10^{-3}$ and (c) $Da = 10^{-2}$.

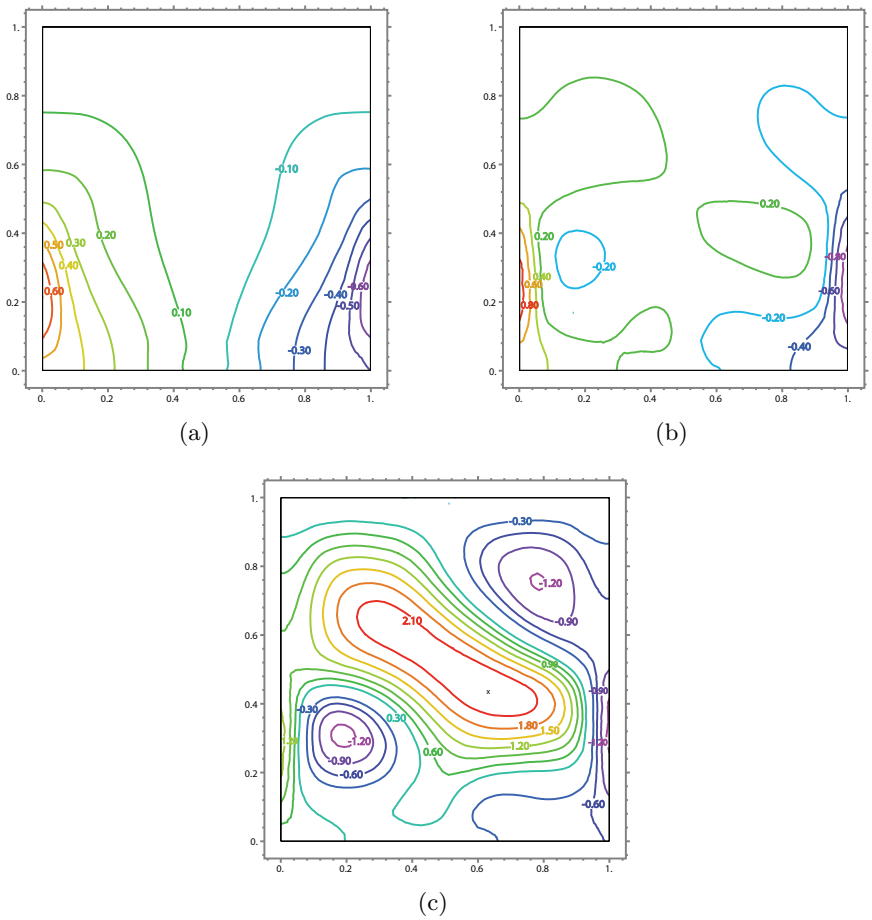

Figure 4: Heatlines for case 1 with $Ra = 10^5$, $Pr = 0.72$ and (a) $Da = 10^{-4}$ (b) $Da = 10^{-3}$ and (c) $Da = 10^{-2}$.

3.2 Case 2

The schematic diagram for case 2 is shown in Figure 1(b). The heat sources are placed at the center portion of the bottom wall ($0.40 \leq X \leq 0.60$) and the lower portion of the side walls ($0.10 \leq Y \leq 0.50$). Detailed computations have been carried out for various $Da = 10^{-4} - 10^{-2}$ with $Ra = 10^5$ and $Pr = 0.72$.

At $Da = 10^{-4}$, values of isotherms at the center core are $\theta = 0.40 - 0.50$ and the isotherms with $\theta = 0.10 - 0.30$ distribute near the bottom corner. Furthermore, the isotherm moves to the top portion of the cavity for $\theta = 0.60$ and moves down to the bottom corner for $\theta = 0.40$ as Da is increased to 10^{-3}. For $Da = 10^{-2}$, value of isotherm with $\theta = 0.40$ moves to the center core of the cavity as seen in Figure 5(c).

At $Da = 10^{-4}$, the multiple circulations are formed in the cavity as seen in Figure 6(a). The maximum value of the primary circulation $|\psi|_{max} = 0.12$. When Da is increased to 10^{-3}, primary circulations in the lower part of the enclosure are stronger than secondary circulations at the upper part which can be seen from the maximum value of the primary circulations $|\psi|_{max} = 0.90$, whereas $|\psi|_{max} = 0.60$ for the secondary circulations. As Da is increased to 10^{-2}, the eye of the primary circulations moves upwards to the upper part of the cavity in Figure 6(c). Moreover, the intensity of fluid motion is stronger with $|\psi|_{max} = 3.00$.

The heatlines emanate from hot surface to cold surface of the vertical walls at $Da = 10^{-4}$. Complex circulations of heatlines are occured in the enclosure and heatlines are wavy near the upper portion of the vertical walls as seen from Figure 7(b) when Da is increased to 10^{-3}. For $Da = 10^{-2}$, the multiple circulations of heatlines are formed in the enclosure and the strength of heat flow is stronger than previous cases with $|\Pi|_{max} = 1.50$.

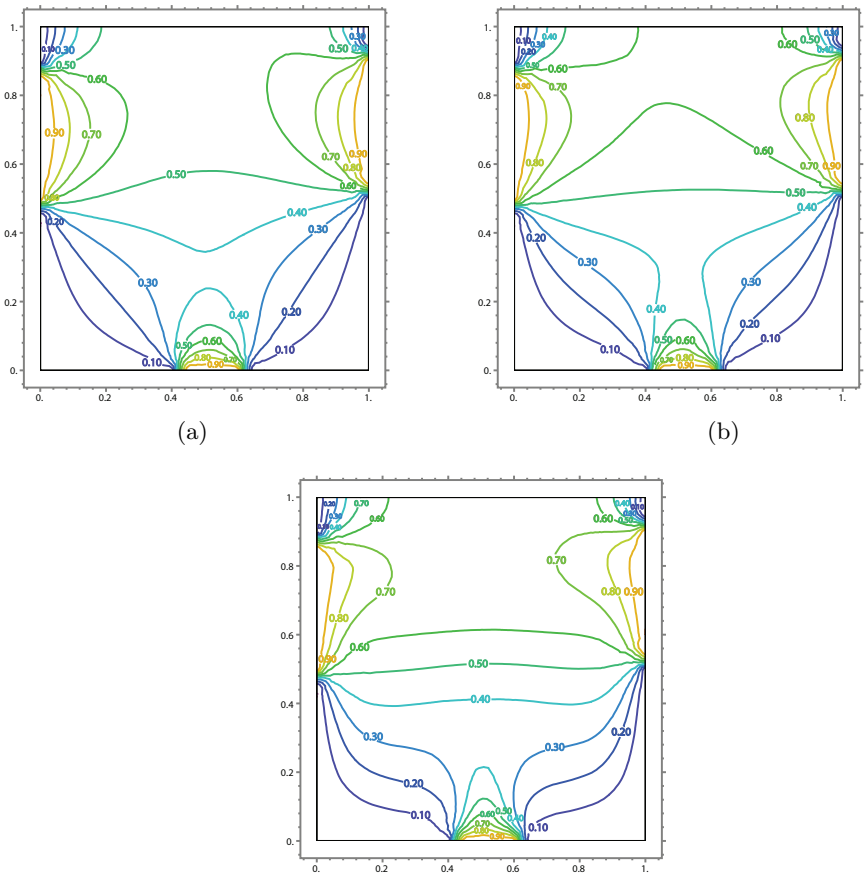

(a) (b)

(c)

Figure 5: Isotherms for case 2 with $Ra = 10^5$, $Pr = 0.72$ and (a) $Da = 10^{-4}$ (b) $Da = 10^{-3}$ and (c) $Da = 10^{-2}$.

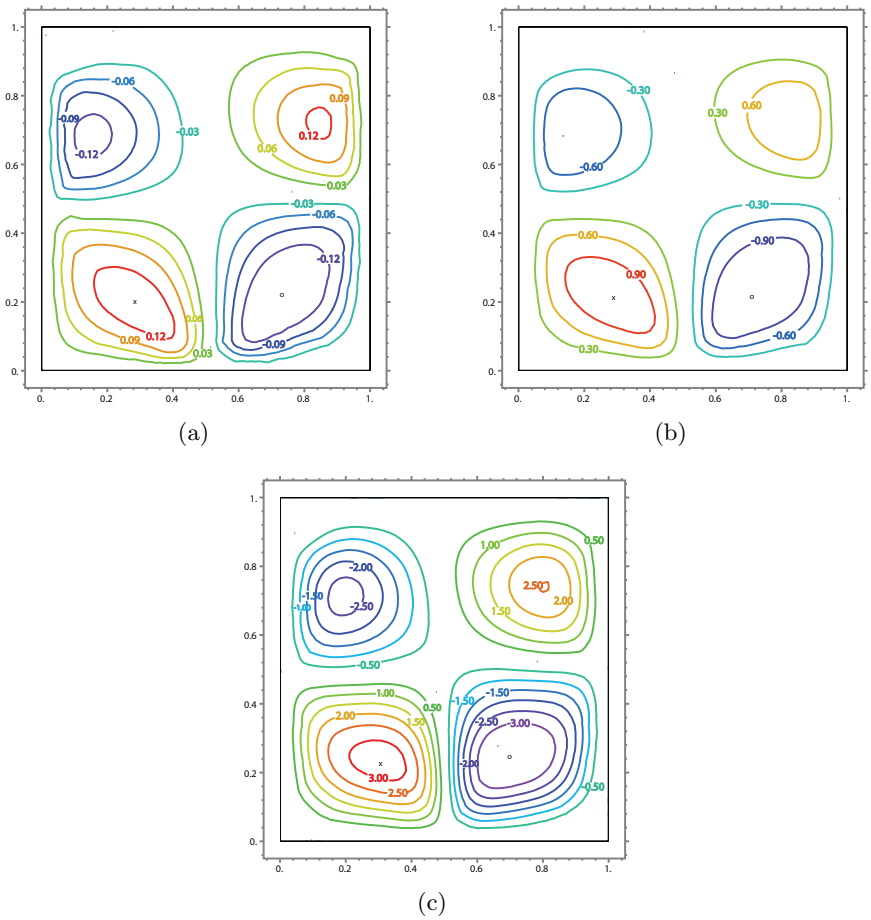

Figure 6: Streamlines for case 2 with $Ra = 10^5$, $Pr = 0.72$ and (a) $Da = 10^{-4}$ (b) $Da = 10^{-3}$ and (c) $Da = 10^{-2}$.

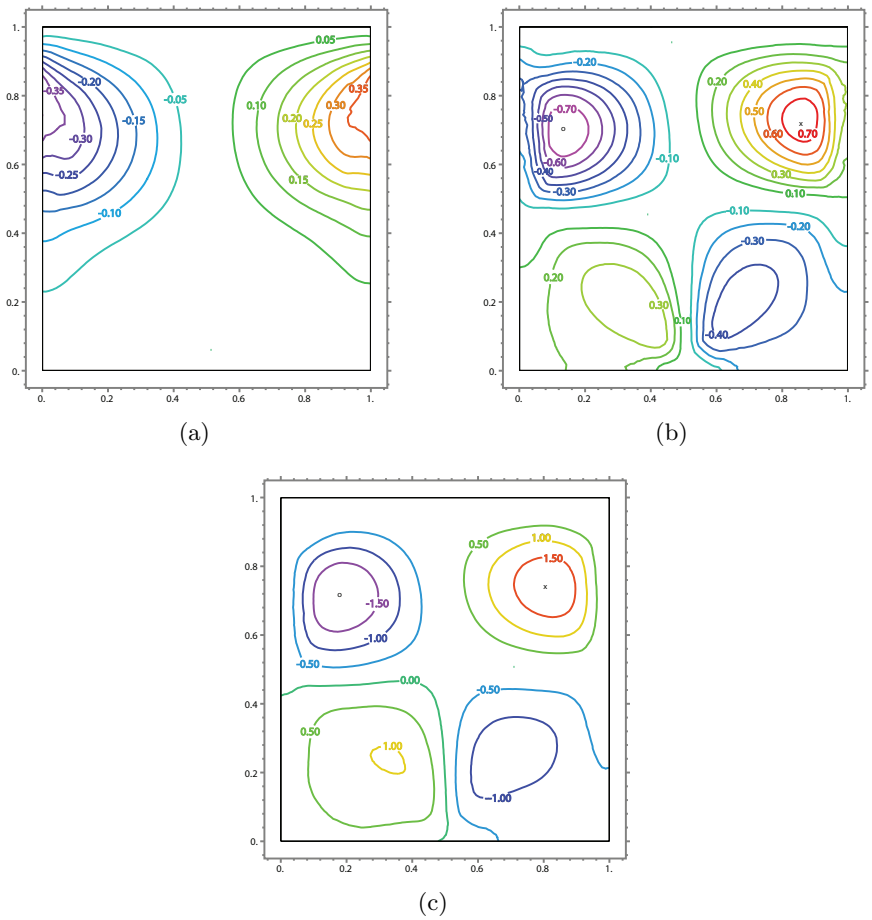

Figure 7: Heatlines for case 2 with $Ra = 10^5$, $Pr = 0.72$ and (a) $Da = 10^{-4}$ (b) $Da = 10^{-3}$ and (c) $Da = 10^{-2}$.

4 Conclutions

Natural convection flow within porous square enclosures is summarized in this section. Two cases are studied by considering various positions of discrete heat sources on the walls. The longer heat sources are placed at the lower portion of the side walls for case 1, while they are placed at the upper portion of the side walls for case 2. The smaller heat source is fixed at the center of the bottom wall for all cases. The parameters for this study are Darcy number ($10^{-4} \leq Da \leq 10^{-2}$), Rayleigh number ($Ra = 10^5$) and Prandtl number ($Pr = 0.72$). The aim of this paper is to examine the effect of varying Da.

From the study results, it is found that the temperature distribution is more distributed in the enclosures when the value of Ra and Pr is kept constant and the values of Da are increased. For flow field, the multiple circulations appear in the cavities and the intensity of fluid flow is stronger as seen from the greater magnitudes of streamfunctions. Thermal mixing in cavities is evaluated by heatlines. In case 1, the heatlines distribute near the lower portion of vertical walls at low Da. For higher Da, the heatlines still distribute near the lower portion of vertical walls and the multiple cells observable. In addition, thermal mixing is intensified which is shown by the formation of heatlines cells. In case 2, the heatlines distribute near the upper portion of vertical walls with low Da. For higher Da, the multiple cells occur in the cavities and thermal mixing is also enhanced due to heat distribution on the walls.

Acknowledgement : This work was supported by Department of Mathematics, Khon Kaen University, Khon Kaen.

References

[1] G. El-Khatib, V. Prasad, Effects of stratification on thermal convection in horizontal porous layers with localized heating from below, Journal of Heat Transfer-Transactions of the ASME 109 (1987) 683–687.

[2] L. Robillard, Multiple steady states in confined porous medium with localized heating from below, Numerical Heat Transfer Part A-Applications 13 (1988) 91–110.

[3] F.C. Lai, C.Y. Choi, F.A Kulacki, Free and mixed convection in horizontal porous layers with multiple heat sources, Journal of Thermophysics and Heat Transfer 4 (1990) 221–227.

[4] F.C. Lai, F.A. Kulacki, Experimental study of free and mixed convection in horizontal porous layers locally heated from below, International Journal of Heat Mass Transfer 4 (1991) 525–541.

[5] T.J. Heindel, F.P. Incropera, S. Ramadhyani, Enhancement of natural convection heat transfer from an array of discrete heat sources, International Journal of Heat Mass Transfer 39 (1996) 479–490.

[6] N.H. Saeid, I. Pop, Natural convection from a discrete heater in a square cavity filled with a porous medium, Journal of Porous Media 8 (2005) 55–63.

[7] F.Y. Zhao, D. Liu, G.F. Tang, Natural convection in a porous enclosure with a partial heating and salting element, International Journal of Thermal Sciences 47 (2008) 569–583.

[8] M. Sankar, Y. Park, J.M. Lopez, Y. Do, Numerical study of natural convection in a vertical porous annulus with discrete heating, International Journal of Heat and Mass Transfer 54 (2011) 1493–1505.

[9] T. Basak, S. Roy, T. Paul, I. Pop, Natural convection in a square cavity filled with porous medium: Effects of various thermal boundary conditions, International Journal of Heat and Mass Transfer 49 (2006) 1430–1441.

[10] R.S. Kaluri, T. Basak, Heatline analysis of thermal mixing due to natural convection in discretely heated porous cavities filled with various fluids, Chemical Engineering Science 65 (2010) 2132–2152.

[11] J.N. Reddy, *An Introduction to the Finite Element Method*, McGraw-Hill, New York, 1993.

[12] T. Basak, S. Roy, Role of Bejans heatlines in heat flow visualization and optimal thermal mixing for differentially heated square enclosures, International Journal of Heat and Mass Transfer 51 (2008) 3486–3503.

[13] R.S. Kaluri, T. Basak, S. Roy, Heatline approach for visualization of heat flow and efficient thermal mixing with discrete heat sources, International Journal of Heat and Mass Transfer 53 (2010) 3241–3261.

(Received 3 April 2012)
(Accepted 30 October 2012)